Comparative Diagenesis and Rare Earth Element Variation in Miocene Invertebrate and Vertebrate Fossils from Panama

Bruce J. MacFadden,[1,*] *Chanika Symister,*[1] *Nicole Cannarozzi,*[1] *Catalina Pimiento,*[1,2,†] *and Carlos DeGracia*[2]

1. Florida Museum of Natural History, University of Florida, Gainesville, Florida 32611, USA; 2. Center for Tropical Paleoecology and Archaeology, Smithsonian Tropical Research Institute, Ancon, Panama

ABSTRACT

The incorporation of rare earth elements (REEs) into the mineral lattices of skeletonized fossils has been used, particularly in vertebrates, to understand diagenesis and other postmortem paleoenvironmental parameters. Little is known about similar processes in invertebrates. Invertebrate and vertebrate fossils were analyzed for REE concentrations and patterns from five Miocene formations in central Panama (~20–6 m.yr. ago). These formations (Culebra, Cucaracha, Gatun, Chucunaque, and Chagres) contain sediments interpreted to range from freshwater to shallow marine environments (depth of <300 m). We also compared different compositional types of fossils, including hydroxylapatite (bone) and aragonite (otoliths) in vertebrates and calcite and aragonite in invertebrates. REEs from modern invertebrates indicate that, as previously reported for vertebrates, invertebrates do not incorporate significant amounts of REEs into their mineral lattices during life; therefore, uptake must primarily occur during diagenesis. Comparisons of REE_N concentrations (REE concentrations normalized to Post-Archean Australian Shale) of the fossils from Panama indicate differences in diagenesis. Within our largest sample from the Gatun Formation, there are significance differences in REE_N concentrations and patterns within different compositional types. For example, shark teeth have the highest REE_N concentrations and otoliths the lowest, with these differences likely a result of physical, chemical, and mineralogical factors. Calcitic and aragonitic fossils from the Gatun Formation show REE_N patterns indicating differential uptake of individual elements during diagenesis. The cerium anomaly, previously used to indicate relative paleobathymetry, did not discriminate water depth in the marine formations. Comparative analysis of REEs in vertebrates and invertebrates provides a powerful tool to understand diagenetic processes, as demonstrated in the five formations and different compositional types studied from the Miocene of Panama.

Online enhancements: supplementary table and figures.

Introduction

Over the past few decades, considerable efforts have been focused on elucidating how rare earth elements (REEs) are incorporated into hard skeletal tissues during fossilization. With regard to vertebrates, this field has proven immensely useful for elucidating taphonomic processes, such as temporal mixing (Trueman and Benton 1997), and it has been used as a proxy for degree of diagenesis (Koenig et al. 2009; MacFadden et al. 2010*a*). Using fossil fish fragments (ichthyoliths) in marine sediments, REEs have been employed as a proxy to understand paleoceanographic parameters, such as paleobathymetry (e.g., Elderfield and Greaves 1982; Elderfield and Pagett 1986; Lécuyer et al. 2004; although see Hewartz et al. 2013). When fossil deposits have taphonomic sorting of multiple depositional events spanning a considerable duration of geological time (e.g., 10^6 yr or more), then comparisons of REEs have been used as a relative dating tool (e.g., Trueman et al. 2005; MacFadden et al. 2007).

Depending on the taphonomic context, vertebrate fossils begin to incorporate REEs into their skeletal elements upon death (Trueman et al. 2004; Tütken et al. 2008). Thereafter, uptake apparently continues for at least 10^3 yr during early diagenesis (Trueman 1999; Patrick et al. 2002). Although the earlier lit-

Manuscript received March 4, 2015; accepted August 28, 2015; electronically published December 3, 2015.

* Author for correspondence; e-mail: bmacfadd@flmnh.ufl.edu.

† Paleontological Institute and Museum, University of Zurich, 8006 Zurich, Switzerland.

[The Journal of Geology, 2015, volume 123, p. 000–000] 0022-1376/2015/12306-00XX$15.00. DOI:10.1086/684006

erature indicated that after this time REE uptake is dramatically reduced or essentially becomes a closed system (Trueman 1999; Patrick et al. 2002), more recent studies have demonstrated that this may not always be the case. Thus, individual REEs may be incorporated in different proportions and at different rates depending on the diagenetic environment (Hewartz et al. 2013; Trueman 2013).

In contrast to the growing body of literature about REE diagenesis of vertebrate skeletal tissues, relatively little is known about this process in either modern or fossil invertebrates and microbiolites. Sholkovitz and Shen (1995) suggested that REEs are incorporated into the aragonitic lattice of four species of modern corals from Bermuda. Webb and Kamber (2000) studied the incorporation of REEs into Holocene reefal microbiolites (stromatolites) and found these organisms, which precipitate high-Mg calcite, to be a more reliable proxy for seawater REE chemistry than skeletal carbonates. Amzy et al. (2011) studied REEs incorporated into modern and ancient brachiopods, which precipitate low-Mg calcite into their skeletons. They found variation in the total amount of REEs (∑REEs) incorporated into modern brachiopod shells that seem to indicate significant uptake in vivo. For example, mean $\sum REE_N$ for cold-water brachiopods was 0.2208 ppm, and mean $\sum REE_N$ for warm-water brachiopods was 0.2492 ppm. With regard to fossils, REEs from Silurian and Eocene brachiopods indicate REE_N trends and cerium anomalies similar to those of modern brachiopods. In contrast to a fairly clear pattern of little uptake of REEs in vivo for vertebrates, the literature for invertebrates remains scarce with regard to the relative incorporation of REEs in vivo and during diagenesis. Furthermore, little has been reported in the literature about the timing and duration of REE uptake in invertebrates during diagenesis. Given the different biomineralogies for invertebrates, it does not necessarily follow that their calcitic and aragonitic skeletal tissues would incorporate REEs during diagenesis in a manner similar to those of the principally phosphatic biominerals in vertebrates.

Given the state of our understanding and few comparative studies across taxonomic and compositional groups, in this study we present new data to demonstrate how REEs are incorporated into vertebrate and invertebrate fossils. We analyze fossils from a ~14-m.yr. sequence of Miocene sediments spanning terrestrial and marine paleoenvironments in Panama. Through the lens of REE proxies, our goals are to understand (1) the variation, comparative rates, and patterns of diagenetic uptake; (2) individual, taxonomic, and mineralogical variation; and (3) potential applications for paleoenvironmental reconstructions within this sequence, particularly related to paleobathymetry.

Brief Review of Biomineralization across Mineralogical and Taxonomic Groups

Five mineralogical types are analyzed below from the sequence in Panama and corresponding modern taxa, that is, not fossilized. These include bioapatite (hydroxylapatite) in vertebrates, calcite in gastropods, high-Mg calcite in echinoderms, aragonite in bivalves, and aragonite in ray-finned bony fish otoliths. As mentioned above, one of the goals for this article is to understand how these different mineralogical types incorporate REEs during diagenesis. This brief review is intended to provide relevant background to frame the results presented below.

Hydroxylapatite. Vertebrate skeletal tissues primarily consist of bone, dentine, and enamel (and related tissues, e.g., enameloid in sharks). Taken together, these are included within the apatite group with the basic chemical formula $Ca_5(PO_4)_6OH_2$, of which the bioapatite variant in fossils is frequently referred to a hydroxylapatite or, in the unaltered state, the mineral variant dahlite. The principal difference in the composition of vertebrate skeletal tissues is the relative percentage of mineral versus organic phases. Bone and dentine consist of about 70%–75% hydroxylapatite, with the remaining ~20% consisting of organics, that is, primarily collagen and water (Carlson 1990). In contrast, enamel consists of more than 95% hydroxylapatite, formed by a dense crystal lattice. This difference in composition as well as physical characteristics (e.g., Trueman 2007; MacFadden et al. 2010*a*) account for widely different diagenetic properties between, for example, the end members porous bone and compact tooth enamel (Trueman and Tuross 2002). With regard to uptake of REEs in vertebrate skeletal tissues during diagenesis, Trueman (2013) presents a comprehensive review of this subject. The REEs analyzed from vertebrate skeletal tissues are generally thought to be incorporated into the mineral lattice by substitution for the Ca^{+2} cation, but it can also occur by other processes, such as surficial adsorption and/or authigenic recrystallization (Trueman 2013).

Calcium Carbonate (Calcite and Aragonite). The remainder of the biominerals studied here are represented by the two minerals calcite and aragonite. Although they have the same composition (i.e., $CaCO_3$), these two minerals are polymorphic, with calcite being hexagonal and aragonite being rhomboidal (Mason and Berry 1968). The relative formation of these two minerals in fossils is related to

multiple factors, including the temperature, pH, and ionic concentrations (e.g., Ca vs. Mg) within the surrounding sedimentary environment as well as inherent vital effects. The fossil and modern invertebrates from Panama studied here consist of two taxa with calcitic skeletons, that is, the bivalve oyster *Hyotissa* (Carter 1990) and echinoderm *Encope*, the latter of which has a characteristic high-Mg content (see Clypeasteridae in Smith 1990). Two other taxa studied here are aragonitic, that is, the gastropod *Strombina* (Bandel 1990) and bony fish otoliths (Francillon-Vieillotet al. 1990; Arslan and Paulson 2003). As will be demonstrated below, each of these $CaCO_3$ skeletal types incorporate REEs during diagenesis, with the principal substitution within the Ca^{+2} site of the crystal lattice. The difference in the relative proportion of the Ca and Mg cations in the calcite as well as the formation of calcite versus aragonite relate to several factors during both the amorphous precursor phase and the crystalline phase of mineral growth (Weiss et al. 2002; Weiner 2008). The reasons for why different taxonomic groups of invertebrates precipitate different varieties of $CaCO_3$ also relate to the availability of Ca and Mg in the ancient oceans (Wilkinson 1979; Balthasar and Cusack 2015) as well as the vital effects of specific groups, such as, for example, the preferential incorporation of relatively high levels of Mg in echinoderms (Rosenberg 1990).

Although vertebrate skeletal tissues are dominantly composed of hydroxylapatite, the notable exception is ray-finned bony fish (Actinopterygii), which precipitate aragonite in their inner ear ossicles (Francillon-Vieillot et al. 1990). These structures, called otoliths, are widely preserved in the fossil record (Nolf 1986). The crystal structure of otolith aragonite is cryptocrystalline, that is, although difficult to determine with X-ray diffraction (XRD), this structure can be observed under high magnification. Like many invertebrates, otoliths grow incrementally and, in conjunction with stable isotopes, have been used to understand ancient and modern ecology (e.g., Francillon-Vieillot et al. 1990; Patterson et al. 1993; Darnaude et al. 2014).

As we will see in our results below, variations in the uptake of REEs into skeletonized tissues across different mineralogical types, taxonomic groups, and timescales studied here are affected differently by diagenetic processes.

Geological Setting and Context

The samples analyzed in this study were collected from the Neogene sequence of sedimentary rocks exposed along the southern portion of the Panama Canal basin (Culebra Cut), from east and west of Colon along the margins of the Caribbean basin (Gatun and Pina, respectively), and from Lake Bayano in eastern Panama (fig. 1). Collectively, the five formations span a temporal range from about 20 to 6 Ma and are briefly described below.

Culebra Formation. The oldest unit represented in our study is the early Miocene Culebra Formation, principally as it is exposed in a ~150-m-thick composite section of marine silts and sands on the west side of the Panama Canal in the Culebra Cut (approximate lat. 9.05°N, long. 79.66°W). The fossils analyzed in this study, which consist of shark teeth (Pimiento et al. 2013*b*), were collected from the uppermost part of the unit, which lies above the prominent Emperador Limestone. Kirby et al. (2008) interpret these upper units to represent distal distributary bars and channels, and thus they were deposited at or near sea level. Although land mammals are sometimes found in this zone (MacFadden et al. 2010*b*), the dominant fossils from the upper Culebra Formation include marine invertebrates and shallow-water sharks (Pimiento et al. 2013*b*). The upper portion of the Culebra Formation in the general zone of the fossils studied here is constrained by Sr ratio age determinations of 19.12 ± 0.42 and 19.83 ± 0.39 Ma (Kirby et al. 2008), indicating an early Miocene age.

Cucaracha Formation. Outcrops of this formation are primarily exposed along the west side of the Panama Canal in the Culebra Cut. Our principal reference section at the Centenario Bridge (lat. 9.03°N, long. 79.64°W) does not expose the contact with the underlying Culebra Formation but is overlain by the basaltic Pedro Miguel Formation. Another important section of the Cucaracha Formation at Hodges Hill includes a vertebrate microfaunal site plus the contact with the underlying Culebra Formation. The Cucaracha Formation is primarily composed of clays but also includes lenticular sands and conglomeratic units. The finer-grained units within the Cucaracha Formation have considerable development of paleosols (Retallack and Kirby 2007). Taken together, a composite section of the Cucaracha Formation spans a thickness of about 140 m (Kirby et al. 2008). An interbedded welded tuff located near the middle of this section has yielded mean radiometric ages of 18.96 ± 0.90 Ma (Ar/Ar) and 18.81 ± 0.30 Ma (U-Pb). Given these constraints and magnetostratigraphic results that yielded a correlation to chron C5Er on the Geomagnetic Polarity Time Scale, the age of the Cucaracha Formation and its contained Centenario Fauna is constrained to an interval between 18.781 and 19.048 Ma. The fauna recovered to date from the Cucaracha Formation is entirely continental and in-

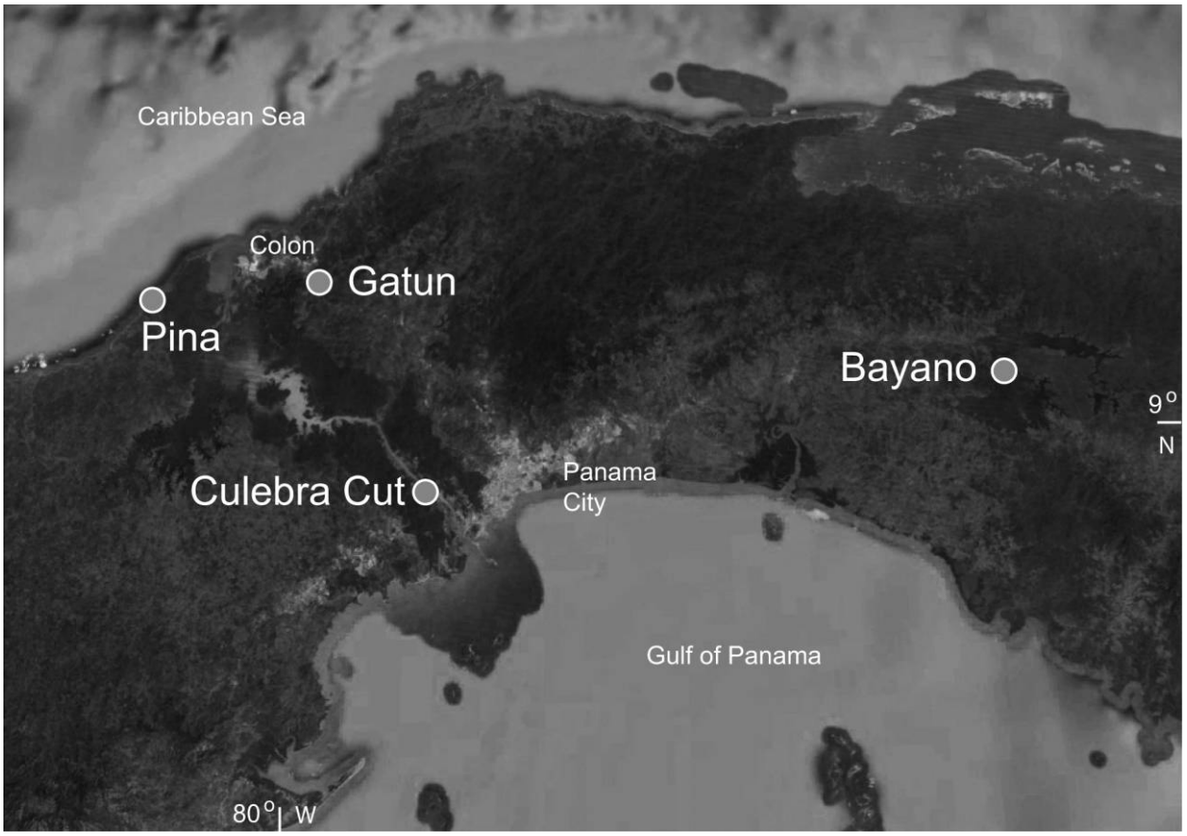

Figure 1. Map (from Google Earth) showing the general localities discussed in the text. A color version of this figure is available online.

cludes an assemblage of land mammals that indicate an early Miocene, early Hemingfordian (He1) North American land mammal age (MacFadden et al. 2014). All other fossil evidence indicates terrestrial and freshwater environments; there are no marine units known from the Cucaracha Formation. Stable isotope ($\delta^{13}C$) data from Centenario mammal teeth are interpreted to represent a range of habitats, from more open woodlands to transitional closed-canopy tropical forests (MacFadden and Higgins 2004). The samples studied here for REE analyses represent bones and teeth of land mammals that were principally collected from 1956 to 1968 and are deposited in the collections of the Smithsonian Institution. On the basis of our fieldwork and background research, these fossils collected a half-century ago approximate the geographic location of the current outcrops of the Cucaracha Formation, as they are exposed several hundred meters north and south of Centenario Bridge (MacFadden 2006; MacFadden et al. 2014).

Gatun Formation. The late Miocene Gatun Formation crops out in the northern part of the Panama Canal basin along the northern margins and adjacent areas of Lake Gatun. The invertebrate faunas from the Gatun Formation have been well known in the literature since the classic monographs by Woodring (1957–1982). The Gatun invertebrate faunas are hyperdiverse, with more than 250 genera of mollusks at some horizons (Jackson et al. 1999). The vertebrates described from the Gatun Formation include sharks (Gillette 1984; Pimiento et al. 2013*a*) and marine mammals (Uhen et al. 2010). A composite stratigraphic section of the Gatun Formation includes about 600 m of fossiliferous volcaniclastic silts and sands (Coates 1999). The invertebrate and vertebrate fossils analyzed in our study come from several localities in the lower 200 m of the composite section, which are between 12 and 10 Ma. The Gatun Formation is typically interpreted to represent relatively shallow marine paleoenvironments (e.g., <100 m; Pimiento et al. 2013*a*), although through detailed stratigraphic analysis Hendy (2013) has demonstrated fine-scale bathymetric fluctuations within this part of the sequence. The Gatun Formation has the largest and most diverse sample of fossils that we analyzed in this study, including sharks, otoliths, the mollusks

Strombina and *Hyotissa*, and the enchinoderm *Encope*. These were collected from four Gatun sublocalities, that is, IDAAN (Instituto de Acueductos y Alcantarillados Nacionales) spoil, Las Lomas (=Sabanitas 01), Texaco, and Isla Payardi (table S1, available online).

Chucunaque Formation. Outcrops of this late Miocene formation are exposed in the Chucunaque/Bayano basin in eastern Panama. Our samples were collected from several exposures of the Chucunaque Formation from Lake Bayano (approximate lat. 9.15°N, long. 78.77°W). Individual outcrops of this formation exposed on islands during seasonally lowered lake levels include massive silty claystones and siltstones. On the basis of calcareous nannofossil and plantonic formaminiferal zonations, the composite age of the Chucunaque Formation ranges from >9.4 to >5.6 Ma (Coates et al. 2004). In addition, new Sr isotope ages at the base of the Chucunaque Formation, which also include the levels from which we collected fossil sharks, further constrain the age, as indicated in figure 2 (Perez et al. 2015). On the basis of evidence from fossil sharks, the paleobathymetry of the Chucunaque Formation is from the littoral zone, with a mean depth of about 100 m (Perez et al. 2015).

Chagres Formation. This formation is exposed west of the Panama Canal along the Caribbean coast, with the fossils that we studied coming from beach outcrops around the town of Pina (approximate lat. 9.282°N, long. 80.047°W). The Chagres Formation, which overlies the Gatun Formation, consists of about 250 m of basal limestone (Toro member) followed by a sequence of massive marine, volcaniclastic sandstones of the Chagres sandstone member (Woodring 1957–1982; Coates and Obando 1996; Collins et al. 1996; Carrillo-Briceño et al. 2015). According to Collins et al. (1996), the Chagres Formation is late Miocene. Of more specific relevance to this study and following the stratigraphic correlations of Coates (1999) and the recent report by Carrillo-Briceño et al. (2015), our location from the upper units at Pina Beach is constrained between 6.4 and 5.8 Ma. Paleobathymetric analysis indicates that the most probable depth of deposition of the Chagres sandstone member at Pina Beach is between 50 and 300 m (Carrillo-Briceño et al. 2015). In this study, we analyzed shark teeth and bone fragments of bony fish.

Material and Methods

REE Analysis: Sample Selection, Preparation, and Analysis. Samples were obtained to determine REEs from modern invertebrate and vertebrate taxa as a control baseline. These samples were compared with fossil invertebrate and vertebrate taxa of Panama from the Miocene sedimentary sequence that includes the Culebra, Cucaracha, Gatun, Chucunaque, and Chagres Formations. To understand possible mineralogical and compositional differences, bones (hydroxylapatite) and otoliths (apatite) were sampled from vertebrate specimens and hard skeleton parts for the invertebrates, representing gastropods (calcite), echinoderms (high-Mg calcite), and bivalves (aragonite). REE analyses were conducted on 89 fossil specimens from collections at the Florida Museum of Natural History, University

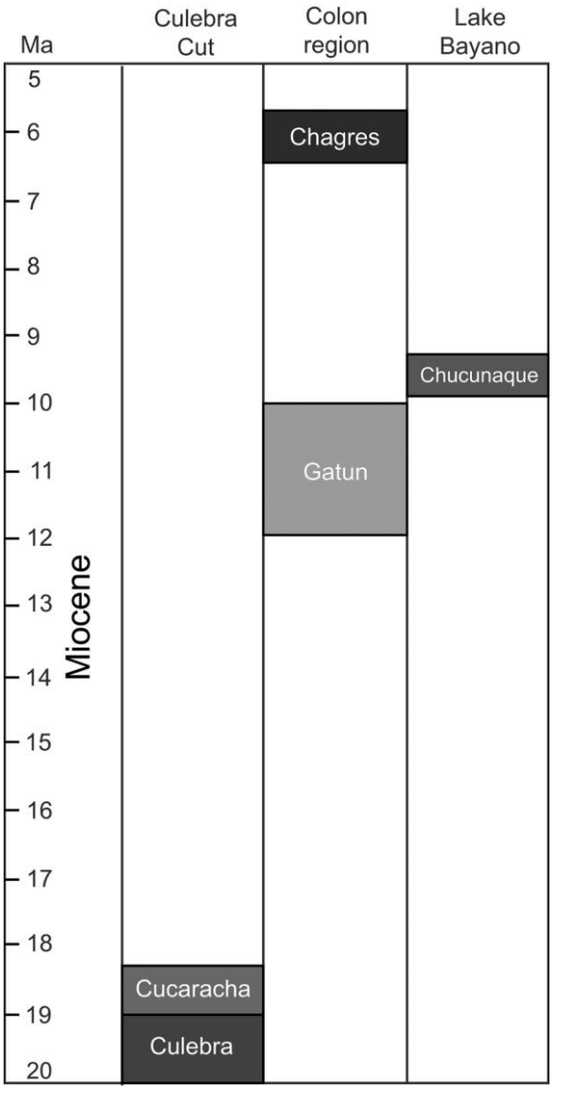

Figure 2. Chart showing the formations described in this article, including the known ages from which samples were analyzed in this study. A color version of this figure is available online.

of Florida (acronym, UF; http://www.flmnh.ufl.edu/collections/databases/), including 17 modern invertebrates (Malacology), 7 modern mammals (Mammalogy), 15 fossil invertebrates (Invertebrate Paleontology), and 51 fossil vertebrates (Vertebrate Paleontology). Stratigraphically, 7 analyses were conducted on specimens from the Culebra Formation, 10 from the Cucaracha Formation, 33 from the Gatun Formation, 8 from the Chucunaque Formation, and 7 from the Chagres Formation, with the remaining 24 analyses representing modern taxa (see table S1 for raw data compilation). Here we use the term "modern" rather than "Recent," because the former implies dried specimens that were never subjected to even the earliest stages of diagenesis (which might be implied if the term "Recent" were used).

After removing about 1 mm of surficial material, about 5–10 mg of sample from each specimen was removed with a Dremel rotary drill. To remove organic matter and other potential contaminants and insoluble residues, these specimen powders were weighed, placed in clean Savillex vials, and dissolved with 2 mL of 8 M HNO_3 overnight on a hotplate. Samples were then opened and dried on the hotplate. Then, 0.8 N HNO_3 spiked with 8-ppb Re was added to the samples to redissolve the dry residue and bring the final dilution to about 2000 ×. The final dilution for trace element analyses was determined by weight for each sample. REE analyses were performed on a Thermo Finnigan ELEMENT 2 inductively coupled plasma mass spectrometer (ICPMS) at the University of Florida Department of Geological Sciences (http://www.geology.ufl.edu/icpmslab.html). All measurements were performed at medium resolution, with Re used as the internal standard. Quantification of results was done by external calibration using a set of gravimetrically prepared REE standards and SRM 1400 (bone ash) standard. The analytical error on the reported REE concentrations is better than 5% on the basis of long-term analyses of USGS standards. Fourteen of the 15 REEs (excluding Pm, $Z = 61$) were analyzed during this procedure. To compensate for the Oddo-Harkins even-odd abundance effect, the REE concentrations reported here are normalized to Post-Archean Australian Shale (PAAS; McLennan 1989) and are indicated by REE_N. In this study, the elements La ($Z = 57$) to Nd ($Z = 60$) are considered light REEs (LREEs), Sm ($Z = 62$) to Tb ($Z = 65$) middle REEs (MREEs), and Dy ($Z = 66$) to Lu ($Z = 71$) heavy REEs (HREEs).

XRD Analysis. After the REE analyses were completed, 8 fossil samples (2 *Encope*, 2 *Hyotissa*, 2 *Strombina*, and 2 otoliths) were selected for XRD analysis to better understand the potential mineralogical changes that had occurred during diagenesis. Each XRD sample was pulverized using a piece of the original fossil in a mortar and pestle. About 0.2 g of the resulting powder was then mounted on a 0-background silica disk and analyzed in the Ultima IV X-ray diffractometer in the University of Florida Department of Geological Sciences. For each sample analysis, the diffractometer was set to run four times each at steps of 0.02°Θ ranging from 20° to 40°, with a 0.5-s step for each interval and 5 revolutions/min for the sample holder. MDI Jade 9 software was used for data reduction and analysis. The interpretation of the peaks also follows Nash et al. (2013) and Xu and Poduska (2014).

Statistics and Data Screening. Statistical analyses of the REE data were done using Statistician (http://www.statisticianaddin.com). Our analysis of the REE data (i.e., normalized to PAAS; McLennan 1989) indicated that they are not normally distributed, although they do not differ from a normal distribution once they are log transformed (supplementary document, available online). Nevertheless, we do not assume normal distributions in our comparisons. Therefore, for each test—whether it be pairwise or multiple ($N > 2$) comparisons—both the parametric test (*t*-test, analysis of variance [ANOVA]) and the equivalent nonparametric test (Wilcoxon, Kruskal-Wallis) were performed on both the original and the log-transformed data set. In almost all cases, the results were the same for both parametric and nonparametric equivalents. Given the distributions of the data sets, in the few cases in which the parametric and nonparametric equivalent test results were different for the null hypothesis, we accepted the decision from the nonparametric test. The median-quartile boxplots were prepared using R (R Development Core Team 2012).

Results and Discussion

Modern versus Fossil REE Signals. Previous research has indicated that modern vertebrate skeletal tissues are essentially devoid of REEs, that is, they are at or below the limits of detectability on the ICPMS. Once the animal dies and its skeleton becomes exposed to taphonomic processes, then REEs can be incorporated within a matter of tens to hundreds of years (Trueman et al. 2004) in terrestrial environments. MacFadden et al. (2010*a*) found that fossil mammal skeletal tissues had between two to three orders of magnitude greater REE concentrations that those of modern mammal specimens. Likewise, Herwartz et al. (2013) found that fossil bone has five orders of magnitude greater concen-

trations of REEs relative to modern bone. In contrast to vertebrates, however, little has been published about REE incorporation into skeletal tissues in vivo and subsequent taphonomic uptake in invertebrate taxa.

For the initial data exploration, ANOVA and Kruskal-Wallis tests of the $\sum REE_N$ and log-transformed $\sum REE_N$ were conducted on the four principal groups of data—that is, fossil invertebrates, fossil vertebrates, modern invertebrates, and modern vertebrates—to test the null hypothesis of no significant differences. The results (table 1; see also fig. 3) indicate that there are significant differences within these groups. Pairwise comparisons were then conducted to determine the source of the significant differences. There was a highly significant ($P \ll 0.01$) difference between two pooled groups representing (1) all fossil invertebrates and vertebrates combined versus (2) all modern invertebrates and vertebrates combined (table 1; fig. 3*A*).

Within subsets of these data, there are no significant differences between the pooled samples of modern invertebrates versus modern vertebrates (table 1). While this may be an artifact of the level of detection available on the ICPMS, the fact that, for example, the modern invertebrates do not have greater concentrations than the vertebrates indicates that both groups likely do not incorporate significant, detectable quantities of REEs into their skeletons in vivo. Comparisons of modern versus fossil vertebrates (fig. 3*B*) confirms what has been stated in the literature (references cited above), namely, that the significantly greater concentrations of REEs in fossils represents uptake during diagenesis. Likewise, the same pattern is seen in a comparison of the invertebrates, with significantly greater concentrations in the fossils relative to modern samples (fig. 3*C*), also indicating uptake during diagenesis. For invertebrates, this is a new result not widely reported in the literature.

Another pattern apparent from our data is that the fossil vertebrate specimens (with $\sum REE_N$ between 10 and 100) indicate at least an order of magnitude greater concentrations relative to those of the fossil invertebrates ($\sum REE_N$ of ~1.0; compare fig. 3*B* with 3*C*). We will further explore these patterns below in our discussion of within-site variation from the Gatun Formation.

Other Sources of Variation. Previous studies have shown that local sedimentary environment can affect the uptake of REEs, that is, that variation can result from differences in pore-water chemistry in different basins that then incorporate individual REEs in different proportions (e.g., Trueman and

Table 1. Parametric and Nonparametric Statistical Comparisons of Representative Groupings of the $\sum REE_N$ and Log-Transformed (LOG) $\sum REE_N$ Data Analyzed in This Study (Also See Table S1)

Group	Test	Critical value (α = .01)	Test statistic	*P*	H_0[a]
Multiple-group comparisons ($N > 2$):					
FI, FV, MI, MV	ANOVA	2.7119	5.3026	.0021	R (S)
LOG FI, LOG FV, LOG MI, LOG MV	ANOVA	2.7119	84.6484	<.0001	R (S)
FI, FV, MI, MV;[b] LOG FI, LOG FV, LOG MI, LOG MV	Kruskal-Wallis	7.8147	62.2724	<.0001	R (S)
Pairwise comparisons ($N = 2$):					
AF vs. AM	*t*	1.1998	4.4130	<.01	R (S)
LOG AF vs. LOG AM	*t*	1.1998	15.4204	<.01	R (S)
AF vs. AR; LOG AF vs. LOG AR	Wilcoxon	2.5758	7.1187	<.0001	R (S)
MI vs. MV	*t*	3.3554	.6896	.5100	N (NS)
LOG MI vs. LOG MV	*t*	3.0123	1.4118	.1815	N (NS)
MI vs. MV; LOG MI vs. LOG MV	Wilcoxon	2.5758	1.3655	.1721	N (NS)
MI vs. FI	*t*	2.9768	5.9787	<.0001	R (S)
LOG MI vs. LOG FI	*t*	2.8073	10.5251	<.0001	R (S)
MI vs. FI; LOG MI vs. LOG FI	Wilcoxon	2.5758	4.7770	<.0001	R (S)
MV vs. FV	*t*	2.6800	4.5945	<.0001	R (S)
LOG MV vs. LOG FV	*t*	3.1058	11.3753	<.0001	R (S)
MV vs. FV; LOG MV vs. LOG FV	Wilcoxon	2.5758	4.1576	<.0001	R (S)

Note. Group abbreviations are as follows: FI = fossil invertebrates; FV = fossil vertebrates; MI = modern invertebrates; MV = modern vertebrates; AF = all fossils (invertebrates and vertebrates combined); AM = all modern (invertebrates and vertebrates combined). ANOVA = analysis of variance; $\sum REE_N$ = total rare earth element concentration normalized to Post-Archean Australian Shale.

[a] Null hypothesis of no difference between or among comparison groups: R = reject, i.e., significant difference (S); N = do not reject, i.e., no significant difference (NS).

[b] Results of original and log-transformed data are the same.

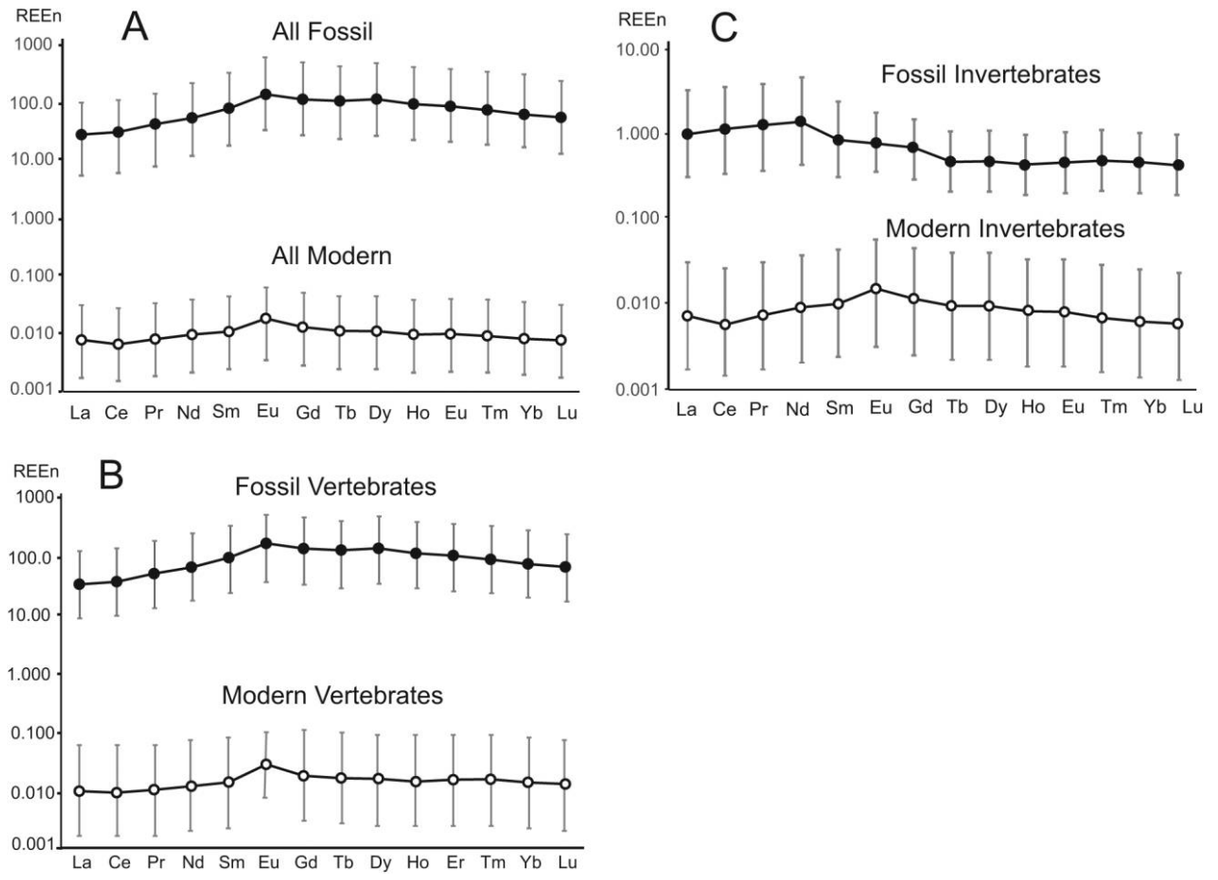

Figure 3. Mean values of fossil versus modern rare earth elements (REEs) for all specimens from Panama analyzed in this study. Shown are comparisons of pooled samples of all modern specimens compared with fossil specimens (*A*), all modern invertebrates compared with fossil invertebrates (*B*), and all modern vertebrates compared with fossil vertebrates (*C*). The error bars indicate 2σ from the mean. Note the changes in the scale of the *Y*-axis in *B* and *C*. REE_N = REE concentration normalized to Post-Archean Australian Shale.

Benton 1997). Our study analyzed REEs from five formations located in different areas within Panama (fig. 1). Our results (table 2) indicate that there are significant differences in the relative REE concentrations from the five formations, which span an interval of 14 m.yr. from early to late Miocene. In contrast to previous assertions that REEs are primarily incorporated into fossil skeletons during early diagenesis, probably ranging from durations of 10^3–10^4 yr (e.g., Patrick et al. 2002), some more recent studies argue that incorporation of REEs during diagenesis can occur over durations of millions of years (see the review in Trueman 2013). As indicated in figure 4, there is a statistically significant general trend toward lower $\sum REE_N$ concentrations with decreasing age, with no overlap between the Culebra and Chucunaque end members. Therefore, on the basis of our samples, the source of the variation in REE concentrations of the fossils is complex and can result from factors such as sedimentary environment, geological time, and (as we will see below) different biomineralogical compositions.

With regard to biomineralogy, from the five formations described above REE samples were obtained on hydroxylapatite (vertebrates), calcite (mollusks), aragonite (vertebrates, bivalves), and high-Mg calcite (echinoderms). To factor out biomineralogy as the primary source of variation in REE concentrations, a second analysis compared only hydroxylapatite in vertebrate samples from the five formations. Likewise, there were significant differences among these samples (fig. 5; table 3). When comparing figures 4 and 5, the general patterns of REE_N are the same, suggesting that the potential differences resulting

Table 2. Parametric and Nonparametric Statistical Comparisons of $\sum REE_N$ and Log-Transformed (LOG) $\sum REE_N$ Data Using Representative Groupings by Formation and Compositional Type (Also See Table S1)

Group	Test	Critical value (α = .01)	Test statistic	P	H_0[a]
All skeletal mineralogies (hydroxylapatite, calcite, aragonite, high-Mg calcite):					
All 5 formations	ANOVA	3.6490	24.3517	<.0001	R (S)
LOG all 5 formations	ANOVA	3.6490	10.9318	<.0001	R (S)
All 5 formations; LOG all 5 formations[b]	Kruskal-Wallis	13.2767	26.6300	<.0001	R (S)
Hydroxylapatite:					
All 5 formations	ANOVA	3.8283	14.5352	<.0001	R (S)
LOG all 5 formations	ANOVA	3.8283	12.7455	<.0001	R (S)
All 5 formations; log all 5 formations	Kruskal-Wallis	13.2767	24.3477	<.0001	R (S)

Note. ANOVA = analysis of variance; $\sum REE_N$ = total rare earth element concentration normalized to Post-Archean Australian Shale.
[a] Null hypothesis of no difference between or among comparison groups: R = reject, i.e., significant difference (S); N = do not reject, i.e., no significant difference (NS).
[b] Results of original and log-transformed data are the same.

from compositional types did not discriminate in this sample. In addition, as described above, variation between and among the five formations can also be a result of differences in geological age, that is, with the older units having greater $\sum REE_N$ concentrations.

Variation within a Taxon: Gatun Formation Sharks. Our REE_N data demonstrate interesting results that relate to variation within compositional groups. For example, there is surprising consistency in how REEs are incorporated into individuals with similar mineralogical compositions. Take, for example, the 13 samples of sharks in which the uptake of REEs are remarkably similar in pattern. This also graphically (fig. 6) shows that in contrast to some previous studies in which the uptake of LREEs tended to be more variable or different from either MREEs or HREEs (e.g., Reynard et al. 1999; MacFadden et al. 2007; Trueman et al. 2011; Hewartz et al. 2013), the amount of variation in, for example, La (LREE), Tb (MREE), and Lu (HREE) are similar. This similarity is also confirmed by ANOVA ($F = 2.0070$, critical = 5.2479, $P = 0.1491$) and Kruskal-Wallis ($\chi^2 = 7.7834$, critical = 9.2103, $P = 0.0204$) results of no significance difference ($\alpha = 0.01$) in the concentration of these three elements within the 13 samples of sharks from the Gatun Formation.

Variation within a Unit: Gatun Formation. One of the goals of this study is to better understand variation in REE uptake within different skeletal materials from a single sedimentary unit. The highly fossiliferous late Miocene Gatun Formation provided the source of these materials, with fossil samples representing hydroxylapatite (bone, $N = 13$), aragonite in both invertebrates (bivalves, $N = 5$) and vertebrates (otoliths, $N = 5$), calcite (gastropods, $N = 5$), and high-Mg calcite (echinoderms, $N = 5$). These samples from the Gatun Formation led us to investigate the following questions: (1) Are differences in REE uptake and concentrations related to mineralogical and compositional groups? (2) Within the groups described above, does porous vertebrate bone, as represented by the shark tooth roots, have relatively high REE concentrations? (3) Within the two different groups that have aragonitic skeletons, if the mineralogies are a dominant factor, then did the vertebrate otoliths and bivalves have similar concentrations and patterns of REE uptake?

A comparison of the five compositional groups from the Gatun Formation indicates different results for the ANOVA relative to the log-transformed and nonparametric tests (fig. 7; table 4). We choose to accept the results of the latter, in which there are highly significant differences ($P < 0.0001$) among the five compositional groups from the Gatun Formation. We interpret the conflicting result of the ANOVA as a type II error (Sokal and Rohlf 1981), in which the null hypothesis (no difference) is accepted although it should be rejected because there are significant differences.

With regard to the five groups analyzed (fig. 7), we find significantly higher concentrations in the shark tooth roots relative to the other four samples (table 4). This confirms previous empirical data (Zanazzo et al. 2007; MacFadden et al. 2010*a*) indicating that porous vertebrate bone, which has a large amount of surface area, is highly prone to diagenesis, as evidenced by the higher REE concentrations. At the other end of the spectrum, the bony fish otoliths have the lowest REE_N concentrations in comparison to the other four compositional and taxonomic groups. This likely reflects their dense, cryptocrystalline matrix, although other organic or inorganic processes (e.g., Elderfield and Graves 1982; Hewarth et al. 2013; Trueman 2013; Lécuyer et al.

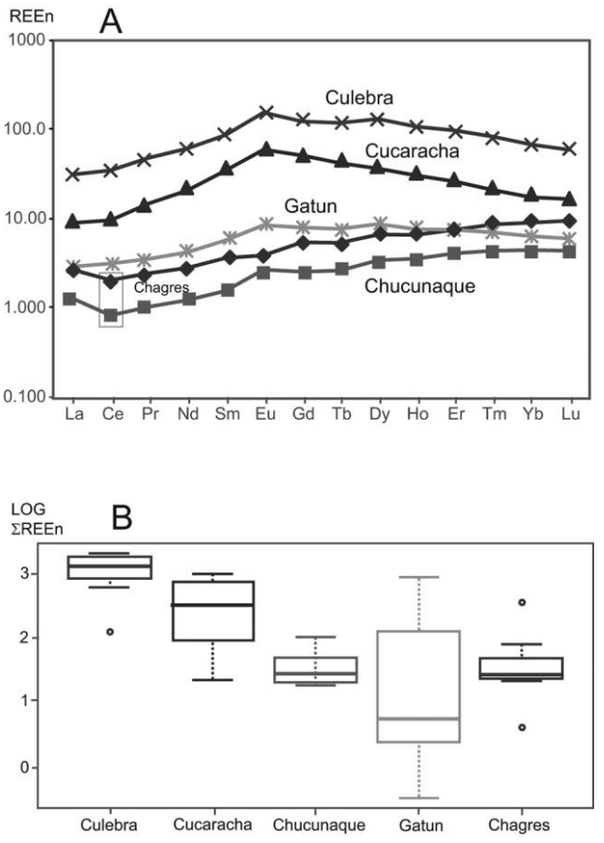

Figure 4. *A*, Mean rare earth element (REE) concentrations and patterns from pooled samples from each of the five formations studied here (i.e., Culebra, Cucaracha, Gatun, Chucunaque, and Chagres). *B*, Median-quartile boxplot of log-transformed (LOG) $\sum REE_N$ by formation. The box including the Ce values from the Chucunaque and Chagres Formations is discussed in the section "REEs as Paleoenvironmental Indicators." REE_N = REE concentration normalized to Post-Archean Australian Shale; $\sum REE_N$ = total REE_N. A color version of this figure is available online.

2014; Schipf et al. 2015) cannot be ruled out without further study. Interestingly, the two groups with aragonitic compositions (otoliths and the gastropod *Strombina*) have significantly different REE_N concentrations, suggesting that the primary determinant is governed by physical, not mineralogical, structure. This is similar to observations of hydroxylapatite in vertebrates wherein teeth, with their more compact structure, typically have lower concentrations than porous bone or other histological types, like dentine (Zanazzo et al. 2007; MacFadden et al. 2010*a*).

So far we have been focused on the $\sum REE_N$ concentrations. As depicted in figure 7, however, the plots show some interesting patterns of REE_N uptake. On the one hand, the hydroxylapatite and calcite (including the high-Mg *Encope*) have REE_N patterns in which the $LREE_N$s (e.g., La) occur at lower concentrations than $HREE_N$s (e.g., Lu). In contrast—and despite the fact that the two aragonitic compositional types have significantly different REE_N concentrations (table 4)—they are consistent in the patterns of REE_N uptake and are different from the hydroxylapatite and calcite skeletal materials. Thus, in the aragonitic shells and otoliths, uptake of $LREE_N$ (e.g., La) occurs at greater concentrations than $HREE_N$ (e.g., Lu). Expressed quantitatively, La/Lu ratios in the otoliths have a mean of 3.28 and *Strombina* has a mean of 6.48, whereas *Encope* has a mean of 0.49, *Hyotissa* has a mean of 0.51, and the sharks have a mean of 0.45 (fig. 8).

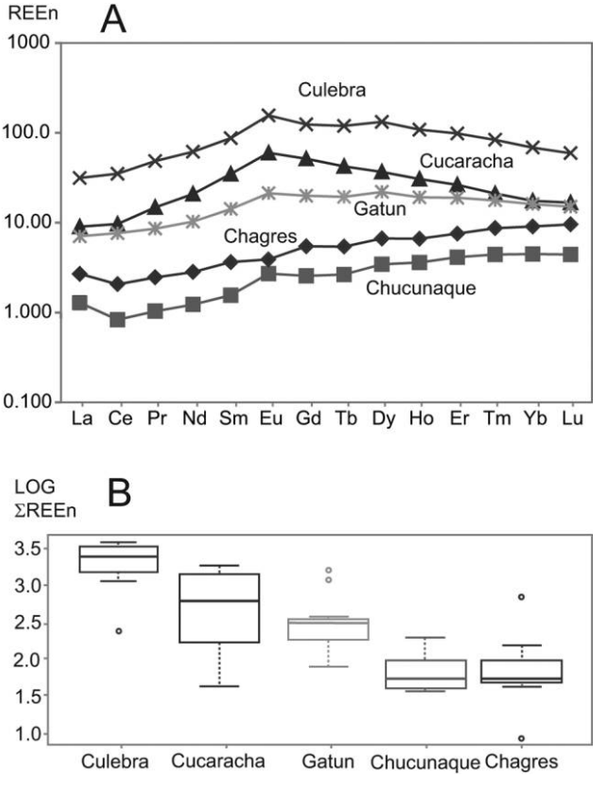

Figure 5. *A*, Mean rare earth element (REE) concentrations for the hydroxylapatite samples from each of the five formations studied here (i.e., Culebra, Cucaracha, Gatun, Chucunaque, and Chagres). *B*, Median-quartile boxplot of log-transformed (LOG) $\sum REE_N$ by formation. REE_N = REE concentration normalized to Post-Archean Australian Shale; $\sum REE_N$ = total REE_N. A color version of this figure is available online.

Table 3. Parametric and Nonparametric Statistical Comparisons of Representative Groupings by Formation and by Formation by Bone of the $\sum REE_N$ and Log-Transformed (LOG) $\sum REE_N$ Data Analyzed in This Study (Also See Table S1)

Group	Test	Critical value (α = .01)	Test statistic	*P*	H_0[a]
All skeletal mineralogies (hydroxylapatite, calcite, aragonite, high-Mg calcite):					
All 5 formations	ANOVA	3.6490	24.3517	<.0001	R (S)
LOG all 5 formations	ANOVA	3.6490	10.9318	<.0001	R (S)
All 5 formations; LOG all 5 formations[b]	Kruskal-Wallis	13.2767	26.6300	<.0001	R (S)
Hydroxylapatite:					
All 5 formations	ANOVA	3.8283	14.5352	<.0001	R (S)
LOG all 5 formations	ANOVA	3.8283	12.7455	<.0001	R (S)
All 5 formations; LOG all 5 formations	Kruskal-Wallis	13.2767	24.3477	<.0001	R (S)

Note. ANOVA = analysis of variance; $\sum REE_N$ = total rare earth element concentration normalized to Post-Archean Australian Shale.
[a] Null hypothesis of no difference between or among comparison groups: R = reject, i.e., significant difference (S); N = do not reject, i.e., no significant difference (NS).
[b] Results of original and log-transformed data are the same.

On the basis of the REE data alone, the explanation for the different patterns of uptake in the hydroxylapatitic and calcitic fossils versus the aragonitic fossils is not clear. We therefore considered two possible explanations: (1) the different patterns of REE_N concentrations result from different relative uptake of individual REEs during early diagenesis or (2) later stages of diagenesis included subsequent uptake that produced different REE_N patterns.

To obtain additional information about the timing of REE_N uptake as it might relate to initial or subsequently altered skeletonized $CaCO_3$ minerals, XRD was performed on two samples each of the otoliths and *Strombina*, both composed of aragonite, and *Encope* and *Hyotissa*, both composed of calcite. With multiple XRD peaks between 26 to 28 2Θ and then at greater than 33 2Θ (fig. 9), the otoliths and *Strombina* are confirmed to be composed of aragonite, whereas with a primary XRD peak between 29 and 30 2Θ, the *Hyotissa* and *Encope* samples are confirmed to be composed of calcite. Interestingly, *Encope*, which is a member of the echinoderm family Cylpeasteridae, a group reported to have a shell consisting of high-Mg calcite, typically has an asymmetrical (right-skewed) calcite peak. This asymmetry is not seen in figure 9*G* and 9*E*, suggesting that the Mg is present in relatively low concentrations (Xu and Poduska 2014). Nevertheless, these XRD data suggest that the fossils analyzed from the Gatun Formation essentially retain their original mineralogy and that uptake of REEs occurred during early diagenesis.

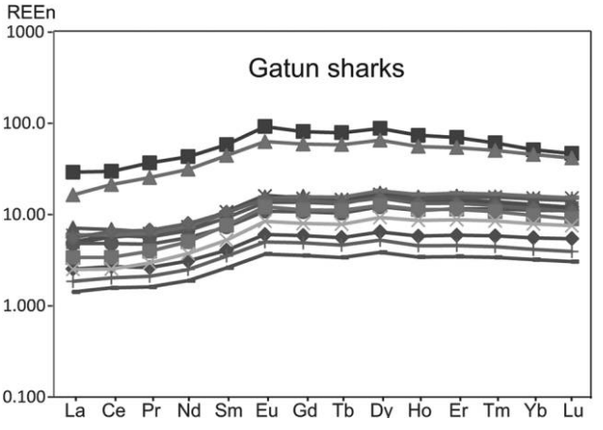

Figure 6. Individual variation within a single taxon and biomineral type, that is, REE_N concentrations of 13 specimens of sharks from the Gatun Formation. REE_N = rare earth element concentration normalized to Post-Archean Australian Shale. A color version of this figure is available online.

REEs as Paleoenvironmental Indicators. A sizeable literature has developed concerning the uptake of REEs during diagenesis in marine environments as paleoenvironmental indicators, for example, in the determination of relative water depth (e.g., see the classic article by Elderfield and Graves 1982; comment by Bender 1982). In particular, the differential incorporation of Ce relative to other REEs has led to the concept of the cerium anomaly as a proxy for relative water depth at the sediment interface. This is usually depicted graphically by lower concentrations of Ce in individual samples relative to other LREEs. Using German and Elderfield (1990), the cerium anomaly (Ce_N/Ce^*) is calculated by

$$\frac{Ce_N}{Ce^*} = \frac{3(Ce_N)}{2La_N + Nd_N}. \quad (1)$$

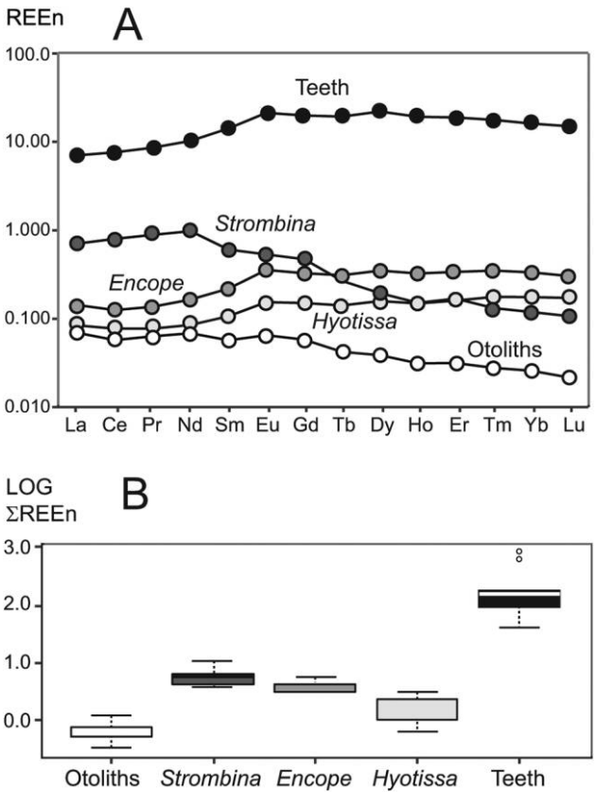

Figure 7. *A*, Mean rare earth element (REE) concentrations from the five compositional groups represented by the Gatun Formation. *B*, Median-quartile boxplot of combined data for each group. LOG = log transformed; REE_N = REE concentration normalized to Post-Archean Australian Shale; $\sum REE_N$ = total REE_N.

We use the cerium anomaly to test previous predictions about relative water depth in the units that we have studied here. On the basis of what is known about the relative water depth of each formation, the REE samples that we analyzed should be ordered as follows: Cucaracha (terrestrial, freshwater), Culebra (estuarine in the zone where we collected samples), and Gatun (shallow water, <50–100 m), with the Chucunaque and Chagres (the latter ~175–300 m) likely representing deeper-water diagenetic processes, although still within the neritic zone.

At first glance, when considering only the mean Ce_N values, the curves for the Chucunaque and Chagres Formations (fig. 4) show a slight negative dip (decreased concentration), suggesting the presence of the cerium anomaly. Nevertheless, once the variation of each formation is taken into consideration, our results (fig. 10) indicate a more complex pattern. For example, fossils from the Cucaracha Formation have a wide degree of variation in the cerium anomaly that do not conform to the patterns seen by the marine units, although this is not surprising because the cerium anomaly does not necessarily pertain to terrestrial paleoenvironmental settings (Bender 1982; Elderfield et al. 1990; Seto and Akagi 2008). Moreover, the other four marine formations also do not conform to the predicted pattern, that is, the Culebra (mean = 0.82) and Gatun (mean = 0.92) Formations should have smaller cerium anomalies relative to the Chucunaque (mean = 0.66) and Chagres (mean = 0.63) Formations, but the reverse is seen in figure 10. We conclude from these data that the cerium anomaly is not a sensitive discriminator of relative water depth in relatively shallow marine systems within the neritic zone (i.e., depths of less than a few hundred meters). On the other hand, our data have considerable variation, but with some populations consisting of small samples ($N = 5$), it is possible that larger samples might result in better statistical discrimination.

Significance and Conclusions

This study presents new data and evidence related to diagenetic variation in a variety of fossil types and biomineral compositions from a 14-m.yr. sequence from Panama. As has been previously shown for vertebrates, our results demonstrate that invertebrates lack detectable quantities of REEs during life and that incorporation of these elements primarily occurs during diagenesis. Within taxa such as the shark teeth from the Gatun, there is surprising uniformity in the uptake of LREEs, MREEs, and HREEs. Taken together for all of the formations and biomineralogical types, the $\sum REE_N$ show a trend related to geological age, suggesting that the substitution of REEs occurs over a considerable period of geological time, that is, on the order of millions of years. In addition, our data also indicate that REE uptake can also relate to sedimentary environment and the physical and chemical characteristics of the different skeletal materials. Thus, considering the sample of biomineralogical types from the Gatun Formation, there is wide variation in both the concentrations and the patterns of REE_Ns. Shark teeth have the highest concentrations and otoliths the lowest; this pattern likely relates to differences in porosity and other physical and mineralogical factors. Fossils with calcitic and hydroxylapatitic hard skeletons differ in patterns of REE_N uptake relative to the aragonitic skeletons in other taxa. XRD results indicate that these patterns represent the original fossil

Table 4. Parametric and Nonparametric Statistical Comparisons for $\sum REE_N$ and Log-Transformed (LOG) $\sum REE_N$ Concentrations and Patterns (La_N/Lu_N) Analyzed in This Study Using Various Combinations of the Five Compositional (Taxonomic) Groups from the Gatun Formation (Also See Table S1)

Group	Test	Critical value (α = .01)	Test statistic	P	H_0[a]
All 5 groups	ANOVA	3.6796	4.0740	.0157	N (NS)
LOG all 5 groups	ANOVA	87.0009	4.0740	<.0001	R (S)
All 5 groups and LOG all 5 groups	Kruskal-Wallis	28.7273	13.2767	<.0001	R (S)
Sharks vs. other 4 groups	*t*	3.0545	3.2257	.0073	R (S)
LOG sharks vs. other 4 groups	*t*	2.7633	13.0587	<.0001	R (S)
Sharks and LOG sharks vs. 4 other groups and LOG 4 other groups	Wilcoxon	2.5758	4.7897	.0008	R (S)
Otoliths vs. other 4 groups	*t*	2.7707	2.8069	.0092	R (S)
LOG otoliths vs. other 4 groups	*t*	2.7633	7.6685	<.0001	R (S)
Otoliths and LOG otoliths compared with 4 other groups[b]	Wilcoxon	2.5758	3.3640	.0008	R (S)
Otoliths vs. *Strombina*	*t*	4.6041	4.4937	.0109	N (NS)[c]
LOG otoliths vs. *Strombina*	*t*	2.3060	7.9803	<.0001	R (S)
Otoliths and LOG otoliths vs. *Strombina*	Wilcoxon	15	40	.0079	R (S)

Note. The groups include sharks (hydroxylapatite, $N = 13$), otoliths (aragonite, $N = 5$), *Strombina* (aragonite, $N = 5$), *Hyotissa* (calcite, $N = 5$), and *Encope* (high-Mg calcite, $N = 5$). ANOVA = analysis of variance; $\sum REE_N$ = total rare earth element concentration normalized to Post-Archean Australian Shale.

[a] Null hypothesis of no difference between or among comparison groups: R = reject, i.e., significant difference (S); N = do not reject, i.e., no significant difference (NS).

[b] Results of original and log-transformed data are the same.

[c] Although not significant at $\alpha = 0.01$, it is significant at $\alpha = 0.05$, as are the log-transformed and the nonparametric equivalent tests.

mineralogy without significant authigenic recrystallization during later stages of diagenesis. We explored cerium anomalies to determine whether our samples would discriminate relative water depth in the marine units, but this is not the case. We found that either (1) cerium anomalies are not a sensitive relative water-depth indicator in shallow marine systems within the neritic zone or (2) our sample sizes are not sufficiently robust to statistically discriminate subtle differences in water depth. In summary, REEs in terrestrial and marine units such as those represented in the Miocene sequence from

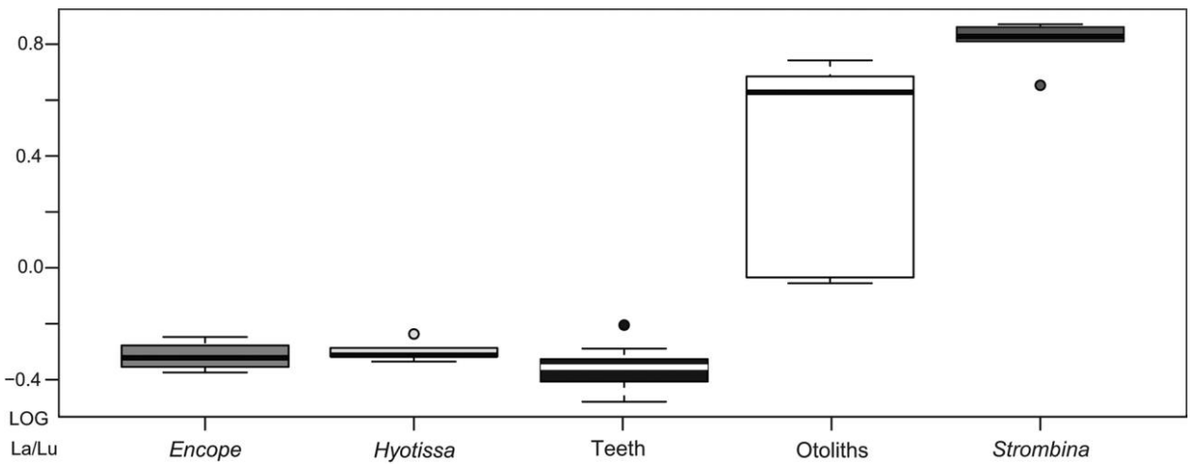

Figure 8. Median-quartile boxplot showing differences in La/Lu ratios of the five compositional types from the Gatun Formation. These ratios, which also represent the different slopes (fig. 5), discriminate the aragonitic mineralogy (otoliths and *Strombina*) from the calcitic (*Encope* and *Hyotissa*) and hydroxylapatitic (sharks) mineralogies. LOG = log transformed.

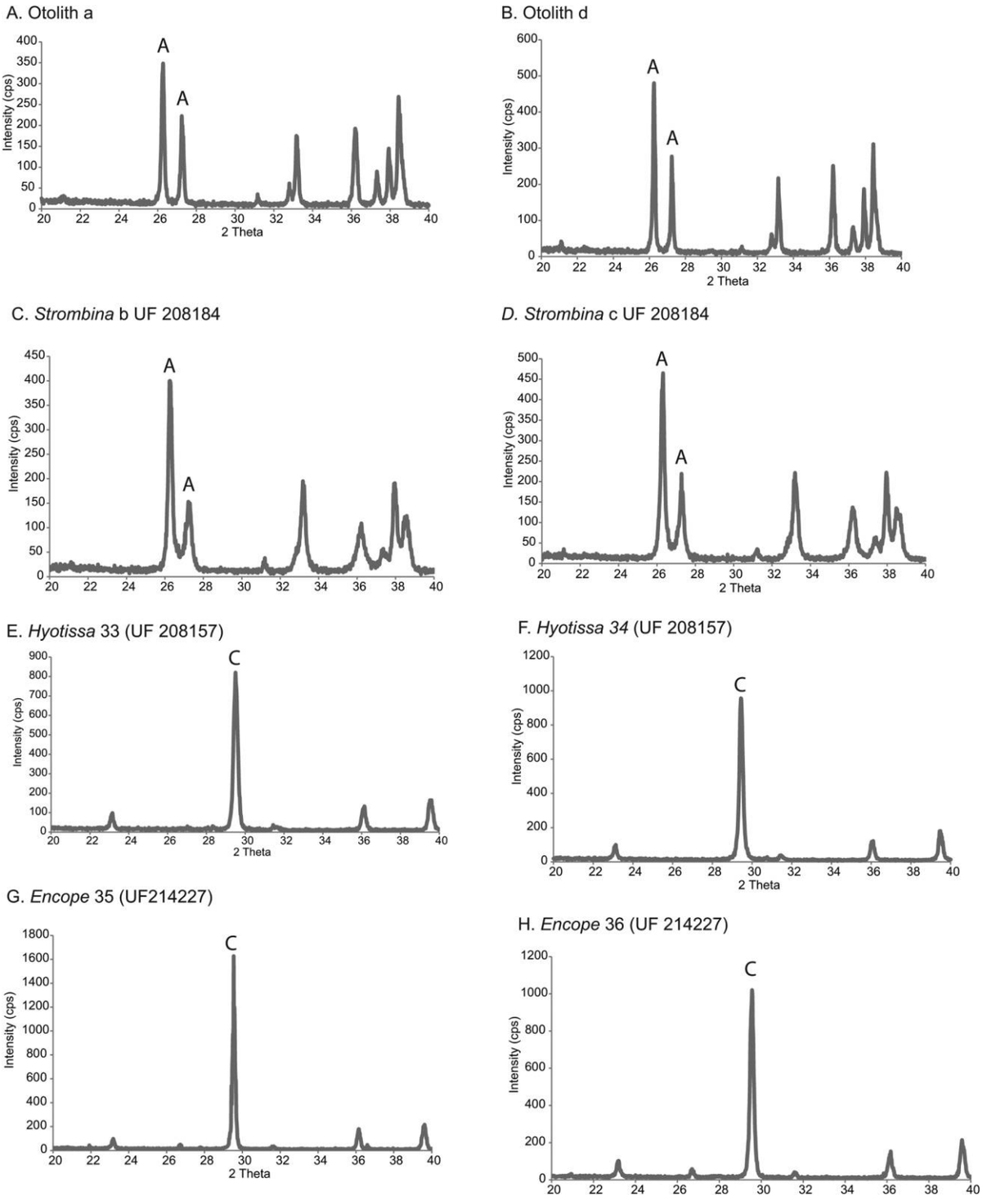

Figure 9. X-ray diffraction patterns for fossils with $CaCO_3$ mineralogy. The otoliths (*A*, *B*) and gastropod *Strombina* (*C*, *D*) have multiple peaks between 26 and 28 2Θ and then at greater than 33 2Θ, indicating aragonite (symbol A on graph). In contrast, the bivalve *Hyotissa* (*E*, *F*) and echinoderm *Encope* (*G*, *H*) show a primary peak between 29 and 30 2Θ, indicating calcite (symbol C on graph). Despite the fact that it is reported in the literature that echinoderms are characterized by high-Mg calcite, the latter calcite peaks do not show the right-skewed asymmetry characterized by high-Mg calcite. A color version of this figure is available online.

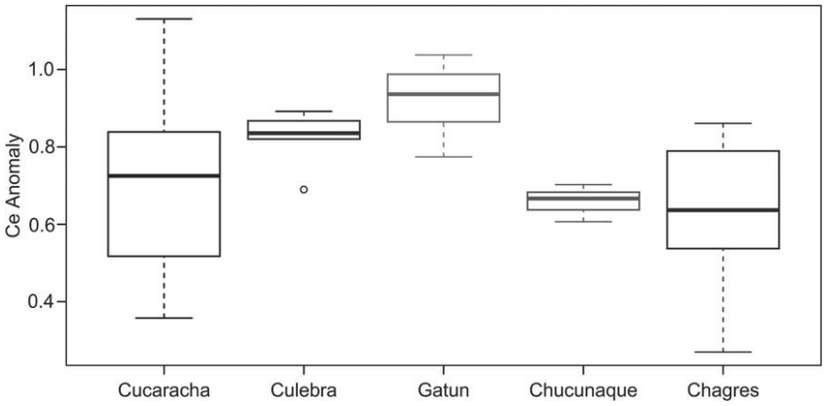

Figure 10. Median-quartile boxplot showing differences in the mean cerium anomaly for fossils from the five formations analyzed in this study. A color version of this figure is available online.

Panama are powerful indicators of diagenetic processes affecting a variety of invertebrate and vertebrate fossils and biomineral compositions.

ACKNOWLEDGMENTS

We thank the curators of fossil collections from the Smithsonian Institution (Paleobiology) and the Florida Museum of Natural History (Invertebrate Paleontology, Malacology, Mammalogy, and Vertebrate Paleontology) who allowed us access to the specimens analyzed here. A. Hendy helped with the selection of modern and fossil invertebrates. We thank G. Kamenov and J. Jaeger of the University of Florida Department of Geological Sciences for help with, respectively, the inductively coupled plasma mass spectrometer (for rare earth element analysis) and the X-ray diffraction laboratory. K. Rohlwing helped with specimen analysis and data reduction. This study benefitted from input provided by and/or discussions with A. Dutton, D. Jones, D. Herwartz, E. Martin, and M. Nash. This research was funded by National Science Foundation grant 0966884 (Office of International Science and Engineering [OISE], Division of Earth Sciences [EAR], Research on Learning in Formal and Informal Settings [DRL]). This is University of Florida Contribution to Paleobiology 685.

REFERENCES CITED

Arslan, K., and Paulson, A. J. 2003. Solid phase extraction for analysis of biogenic carbonates by electrothermal vaporization inductively coupled plasma mass spectrometry (ETV-ICP-MS): an investigation of rare earth element signatures in otolith microchemistry. Anal. Chim. Acta 476:1–13.

Azmy, K.; Brand, U.; Sylvester, P.; Gleeson, S. A.; Logan, A.; and Bitner, M. A. 2011. Biogenic and abiogenic low-Mg calcite (bLMC and aLMC): evaluation of seawater-REE composition, water masses and carbonate diagenesis. Chem. Geol. 280:180–190.

Balthasar, U., and Cusack, M. 2015 Aragonite-calcite seas—quantifying the gray areas. Geology 43:99–102.

Bandel, K. 1990. Shell structure of the Gastropoda and Archaeogastropoda. *In* Carter, J. G., ed. Skeletal biomineralization: patterns, processes and evolutionary trends (Vol. 1). New York, Van Nostrand Reinhold, p. 117–134.

Bender, M. L. 1982. Trace elements and ocean chemistry. Nature 296:203–204.

Carlson, S. J. 1990. Vertebrate dental structures. *In* Carter, J. G., ed. Skeletal biomineralization: patterns, processes and evolutionary trends (Vol. 1). New York, Van Nostrand Reinhold, p. 363–389.

Carrillo-Briceño, J. D.; De Gracia, C.; Pimiento, C.; Aguilera, A. A.; Kindlimann, R.; Santamarina, P.; and Jaramillo, C. 2015. A new late Miocene chondrichthyan assemblage from the Chagres Formation, Panama. J. S. Am. Earth Sci. 60:56–70.

Carter, J. G. 1990. Shell microstructural data for the Bivalvia. Part IV. Order Ostreoida. *In* Carter, J. G., ed. Skeletal biomineralization: patterns, processes and evolutionary trends (Vol. 1). New York, Van Nostrand Reinhold, p. 471–530.

Coates, A. G. 1999. Lithostratigraphy of the Neogene strata of the Caribbean coast, from Limon, Costa Rica, to Colon, Panama. *In* Collins, L. S., and Coates, A. G., eds. A paleobiotic survey of Caribbean faunas from the Neogene of the Isthmus of Panama. Bulletins of American Paleontology. Ithaca, NY, Paleontological Research Institution, p. 16–40.

Coates, A. G.; Collins, L. S.; Aubry, M.-P.; and Berggren, W. A. 2004. The geology of the Darien, Panama, and the late Miocene–Pliocene collision of the Panama arc with northwestern South America. Bull. Geol. Soc. Am. 116:1327–1344.

Coates, A. G., and Obando, J. A. 1996. The geologic evolution of the Central American isthmus. *In* Jackson, J. B. C., et al., eds. Evolution and environment in tropical America. Chicago, University of Chicago Press, p. 21–56.

Collins, L. S.; Coates, A. G.; Berggren, W. A.; Aubry, M.-P.; and Zhang, J. 1996. The late Miocene Panama isthmian strait. Geology 24:687–690.

Darnaude, A. M.; Sturrock, A.; Trueman, C. M.; Mouillot, D.; Campana, S. E.; and Hunter, E. 2014. Listening in on the past: what can otolith $\delta^{18}O$ values really tell us about the environmental history of fishes? PLoS ONE 9:e108539.

Elderfield, H., and Greaves, M. J. 1982. The rare earth elements in seawater. Nature 296:214–219.

Elderfield, H., and Pagett, R. 1986. Rare earth elements in ichthyoliths: variations with redox conditions and depositional environment. *In* Riley, J. P., ed. Sci. Total Environ. 49:175–197.

Elderfield, H.; Upstill Goddard, R.; and Sholkovitz, E. R. 1990. The rare earth elements in rivers, estuaries and coastal seas and their composition of ocean waters. Geochim. Cosmochim. Acta 54:971–991.

Francillon-Vieillot, H.; de Buffrénil., V.; Castanet, J.; Géraudie, J.; Meunier, F. J.; Sire, J. Y.; Zylberberg, L.; and de Ricqlès, A. 1990. Microstructure and mineralization in vertebrate skeletal tissues. *In* Carter, J. G., ed. Skeletal biomineralization: patterns, processes and evolutionary trends (Vol. 1). New York, Van Nostrand Reinhold, p. 471–530.

German, C. R., and Elderfield, H. 1990. Application of the Ce anomaly as a paleoredox indicator: the ground rules. Paleoceanography 5:823–833.

Gillette, D. D. 1984. A marine ichthyofauna from the Miocene of Panama, and the Tertiary Caribbean Faunal Province. J. Vertebr. Paleontol. 4:172–186.

Hendy, A. J. W. 2013. Spatial and stratigraphic variation of marine paleoenvironments in the middle-upper Miocene Gatun Formation, Isthmus of Panama. Palaios 28: 210–227.

Herwartz, D.; Tütken, T.; Jochum, K. P.; and Sander, P. M. 2013. Rare earth elemental systematics of fossil bone revealed by LA-ICPMS analysis. Geochim. Cosmochim. Acta 103:161–183.

Jackson, J. B. C.; Todd, J. A.; Fortunato, H.; and Jung, P. 1999. Diversity and assemblages of Neogene Caribbean Mollusca of lower America. *In* Collins, L. S., and Coates, A. G., eds. A paleobiotic survey of Caribbean faunas from the Neogene of the Isthmus of Panama. Bulletins of American Paleontology. Ithaca, NY, Paleontological Research Institution, p. 193–230.

Kirby, M. X.; Jones, D. S.; and MacFadden, B. J. 2008. Lower Miocene stratigraphy along the Panama Canal and its bearing on the Central American peninsula. PLoS ONE 3:e2791.

Koenig, A. E.; Rogers, R. R.; and Trueman, C. N. 2009. Visualizing fossilization using laser ablation–inductively coupled plasma-mass spectrometry maps of trace elements in late Cretaceous bones. Geology 37:511–514.

Lécuyer, C.; Reynard, B.; and Grandjean, P. 2004. Rare earth element evolution of Phanerozoic seawater recorded in biogenic apatites. Chem. Geol. 204:63–102.

———. 2014. Rare earth element evolution of Phanerozoic seawater recorded in biogenic apatities. Chem. Geol. 204:63–102.

MacFadden, B. J. 2006. North American land mammals from Panama. J. Vertebr. Paleontol. 26:720–734.

MacFadden, B. J.; Bloch, J. I.; Evans, H.; Foster, D. A.; Morgan, G. S.; Rincon, A.; and Wood, A. R. 2014. Temporal calibration and biochronology of the Centenario Fauna, early Miocene of Panama. J. Geol. 112: 113–135.

MacFadden, B. J.; DeSantis, L. R. G.; Labs Hochstein, J.; and Kamenov, G. D. 2010*a*. Physical properties, geochemistry, and diagenesis of xenarthran teeth: prospects for interpreting the paleoecology of extinct species. Palaeogeogr. Palaeoclimatol. Palaeoecol. 291: 180–189.

MacFadden, B. J., and Higgins, P. 2004. Ancient ecology of 15-million-year-old browsing mammals within C3 plant communities from Panama. Oecologia 140: 169–182.

MacFadden, B. J.; Kirby, M. X.; Rincon, A.; Montes, C.; Moron, S.; Strong, N.; and Jaramillo, C. 2010*b*. Extinct peccary "*Cynorca*" *occidentale* (Tayassuidae, Tayassuinae) from the Miocene of Panama and correlations to North America. J. Paleontol. 84:288–298.

MacFadden, B. J.; Labs-Hochstein, J.; Hulbert, R. C., Jr.; and Baskin, J. A. 2007. Revised age of the late Neogene terror bird (*Titanis*) in North America during the Great American Interchange. Geology 35:123–126.

Mason, B., and Berry, L. G. 1968. Elements of mineralogy. San Francisco, Freeman, 550 p.

McLennan, S. M. 1989. Rare earth elements in sedimentary rocks: influence of provenience and sedimentary processes. *In* Lipkin, B. R., and McKay, G. A., eds. Geochemistry and mineralogy of rare earth elements. Reviews in Mineralogy. Washington, DC, Mineralogical Society of America, p. 169–200.

Nash, M. C.; Opdyke, B. N.; Wu, Z.; Xu, H.; and Trafford, J. M. 2013. Simple X-ray diffraction techniques to identify Mg calcite, dolomite, and magnesite in tropical coralline algae and assess peak asymmetry. J. Sed. Res. 83:1084–1098.

Nolf, D. 1986. Otolithi piscium. *In* Schultze, H. P., ed. Handbook of paleoichthyology (Vol. 10). Stuttgart, Fisher, 145 p.

Patrick, D.; Martin, J. E.; Parris, D. C.; and Grandstaff, D. E. 2002. Rare earth element signatures of fossil vertebrates compared with lithostratigraphic subdivisions of the Upper Cretaceous Pierre Shale, central South Dakota. Proc. S. D. Acad. Sci. 81:161–179.

Patterson, W. P.; Smith, G. R.; and Lohmann, K. C. 1993. Continental paleothermometry and seasonality using the isotopic composition of aragonitic otoliths of fresh-

water fishes. *In* Swart, P. K.; Lohmann, K. C.; Mckenzie, J.; and Savin, S., eds. Climate change in continental isotopic records. Washington, DC, American Geophysical Union, doi:10.1029/GM078p0191.

Perez, V.; Hendy, A.; MacFadden, B.; Gonzalez-Barba, G.; and Hubbell, G. 2015. Late Miocene chondrichthyans from Lago Bayano, Panama with implications for a marine connection between the Caribbean and Pacific. Geol. Soc. Am. Abstr. Programs, Baltimore, MD (November 1–4). Vol. 47, paper 193-7.

Pimiento, C.; Gonzalez-Barba, G.; Ehret, D. J.; Hendy, A. J.; MacFadden, B. J.; and Jaramillo, C. 2013*a*. Sharks and rays (Chondrichthyes, Elasmobranchii) from the last Miocene Gatun Formation of Panama. J. Paleontol. 87:755–774.

Pimiento, C.; Gonzales, G.; Hendy, A.; Jaramillo, C.; MacFadden, B. J.; Montes, C.; Suarez, S.; and Shippritt, M. 2013*b*. Early Miocene chondrichthyes from the Culebra Formation, Panama: a window into marine vertebrate faunas before closure the Central American Seaway. J. S. Am. Earth Sci. 42:159–170.

Retallack, G. J., and Kirby, M. X. 2007. Middle Miocene global change and paleogeography of Panama. Palaios 22:667–679.

Reynard, B.; Lécuyer, C.; and Grandjean, P. 1999. Crystal-chemistry controls on rare-earth element concentrations in fossil biogenic apatites and implications for paleoenvironmental reconstructions. Chem. Geol. 155:233–241.

R Development Core Team. 2012. R: a language and environment for statistical computing. Vienna, R Foundation for Statistical Computing. www.r-project.org.

Rosenberg, G. 1990. The "vital effect" on skeletal trace element content as exemplified by magnesium. *In* Carter, J. G., ed. Skeletal biomineralization: patterns, processes and evolutionary trends (Vol. 1). New York, Van Nostrand Reinhold, p. 567–577.

Schijf, J.; Christenson, E.; and Byrne, R. H. 2015. YREE scavenging in seawater: a new look at an old model. Mar. Chem., forthcoming.

Seto, M., and Akagi, T. 2008. Chemical condition for the appearance of a negative Ce anomaly in streamwaters and ground waters. Geochem. J. 42:371–380.

Sholkovitz, E., and Shen, G. T. 1995. The incorporation of rare earth elements in modern coral. Geochim. Cosmochim. Acta 59:2749–2756.

Smith, A. B. 1990. Biomineralization in echinoderms. *In* Carter, J. G., ed. Skeletal biomineralization: patterns, processes and evolutionary trends (Vol. 1). New York, Van Nostrand Reinhold, p. 413–443.

Sokal, R. P., and Rohlf, F. J. 1981. Biometry. San Francisco, Freeman, 859 p.

Trueman, C. 1999. Rare earth element geochemistry and taphonomy of terrestrial vertebrate assemblages. Palaios 14:555–568.

———. 2007. Trace element geochemistry of bonebeds. *In* Rogers, R. R.; Eberth, D. A.; and Fiorillo, A. R., eds. Bonebeds: genesis, analysis, and paleobiological significance. Chicago, University of Chicago Press, p. 397–435.

———. 2013. Chemical taphonomy of biomineralized tissues. Palaeontology 56:475–486.

Trueman, C. N. G.; Behrensmeyer, A. K.; Tuross, N.; and Weiner, S. 2004. Mineralogical and compositional changes in bones exposed on soil surfaces in Amboseli National Park, Kenya: diagenetic mechanisms and the role of sediment pore fluids. J. Archaeol. Sci. 31:721–739.

Trueman, C. N., and Benton, M. J. 2007. A geochemical method to trace the taphonomic history of reworked bones in sedimentary settings. Geology 25:263–266.

Trueman, C. N. G.; Field, J. H.; Dortch, J.; Charles, B.; and Wroe, S. 2005. Prolonged coexistence of humans and megafauna in Pleistocene Australia. Proc. Natl. Acad. Sci. U.S.A. 102:8381–8385.

Trueman, C. N.; Kocsis, L.; Palmer, M.; and Dewdney, C. 2011. Fractionation of rare earth elements within bone mineral: a natural cation exchange system. Palaeogeogr. Palaeoclimatol. Palaeoecol. 310:124–132.

Trueman, C. N., and Tuross, N. 2002. Trace elements in Recent and fossil bone apatite. *In* Kohn, M. J.; Rakovan, J.; and Hughes, J. M., eds. Phosphates: geochemical, geobiological, and materials importance. Rev. Mineral. Geochem. 48:489–521.

Tütken, T.; Vennemann, T. W.; and Pfretzschner, H.-U. 2008. Early diagenesis of bone and tooth apatite in fluvial and marine settings: constraints from combined oxygen isotope, nitrogen and REE analysis. Palaeogeogr. Palaeoclimatol. Palaeoecol. 266:254–268.

Uhen, M. D.; Coates, A. G.; Jaramillo, C. A.; Montes, C.; Pimiento, C.; Rincon, A.; Strong, N.; and Velez-Juarbe, J. 2010. Miocene mammals from the Miocene of Panama. J. S. Am. Earth Sci. 30:167–175.

Webb, G. E., and Kamber, B. S. 2000. Rare earth elements in Holocene microbialites: a new shallow seawater proxy. Geochim. Cosmochim. Acta 64:1557–1565.

Weiner, S. 2008. Biomineralization: a structural perspective. J. Struct. Biol. 163:229–234.

Weiss, I. M.; Tuross, N.; Addadi, L.; and Weiner, S. 2002. Mollusk larval shell formation: amorphous calcium carbonate is a precursor for aragonite. J. Exp. Zool. 293:478–491.

Wilkinson, B. H. 1979. Biomineralization, paleoceanography, and the evolution of calcareous marine organisms. Geology 7:524–527.

Woodring, W. P. 1957–1982. Geology and paleontology of Canal Zone and adjoining parts of Panama. U.S. Geol. Surv. Prof. Pap. 306-A to 306-F, 759 p.

Xu, B., and Poduska, K. M. 2014. Linking crystal structure with temperature-sensitive vibrational models in calcium carbonate minerals. Phys. Chem. Chem. Phys. 16: 17,635–17,639.

Zanazzo, A.; Kohn, M. J.; MacFadden, B. J.; and Terry, D. O. 2007. Large temperature drop across the Eocene-Oligocene transition in central North America. Nature 445:639–642.